Numerical investigation of cement sheath integrity under thermo-mechanical coupling based on damage mechanics

Chenwang Gu
College of Petroleum Engineering, China University of Petroleum (Beijing), Beijing, China

Yongcun Feng
College of Petroleum Engineering, China University of Petroleum (Beijing), Beijing, China

Nan Chen
Pengbo Operating Company of CNOOC (China) Co., Ltd., Tianjin, China

Xiaorong Li
College of Safety and Ocean Engineering, China University of Petroleum (Beijing), Beijing, China

Jingen Deng
College of Petroleum Engineering, China University of Petroleum (Beijing), Beijing, China

ABSTRACT: The transient changes of pressure and temperature in the wellbore during fracturing could cause cement sheath damage and micro-annulus. In this work, a plastic damage model that considers both damage and yielding is used to describe the full stress-strain mechanical properties of the actual cement sheath. A novel numerical model was established to evaluate the cement sheath integrity considering thermo-mechanical coupling. This model is validated by the laboratory experiment and shows high accuracy. The results indicate that tensile damage occurs inside the cement sheath during the fracturing process, and the maximum damage occurs in the direction of the maximum horizontal stress. The micro-annulus rapidly appears at the first cement sheath interface during depressurization process after injection, which can reach 39.57 μm. With the increase of shutdown time, the micro-annulus gradually decreases. This work reveals the cement sheath failure mechanism and provides a basis for wellbore integrity control.

Keywords: Cement sheath, Thermo-mechanical coupling, Plastic damage, Micro-annulus.

1 INTRODUCTION

Cement sheath integrity is critical to oil and gas development. In the process of hydraulic fracturing, thermal oil recovery, the cement sheath is usually exposed to fluctuating high-pressure and high-temperature environments, which can easily damage and destroy the cement(De Andrade & Sangesland, 2016a; Thiercelin et al., 1998). It is reported that 79.524% of the wells showed sustained casing pressure problems in the Fuling shale gas field in Sichuan, China(Guo et al., 2018; Li et al., 2020; Yan et al., 2018). Therefore, understanding the mechanisms of cement sheath damage under different operating conditions is essential to evaluate wellbore integrity better.

Several cement sheath integrity models under temperature and pressure have been developed. In previous studies, ideal elastic-plastic models have been used to describe the stress-strain characteristics of cement sheath. The Mohr-Coulomb or Drucker-Prager criterion has been used to determine whether the cement has yielded(De Andrade & Sangesland, 2016b; Feng et al., 2017; Gu et al., 2022). The actual cement stone has a large number of internal micro-cracks and micro-voids. The size and distribution of the micro-cracks change under the action of temperature and pressure,

which is characterised by macroscopic degradation of the cement stiffness(Arjomand et al., 2018). Therefore, the conventional ideal elastic-plastic constitutive model can not represent the damage properties of the cement sheath effectively.

Based on thermal-mechanical coupling theory, a numerical model for evaluating the sealability of cement sheath was constructed. The plastic damage model is used considering cement damage and post-yield stress-strain relationship. The temperature and stress distribution of the cement sheath at different times were studied, and the damage mechanism and interface debonding were revealed.

2 MODEL THEORY

2.1 Coupled thermal-stress analysis of wellbore

The stress and temperature fields affect each other, and therefore a fully coupled thermal stress analysis is required. Using a backward-differential approach, the temperature is integrated, and Newton's method is used to solve the nonlinear coupled equation:

$$\begin{bmatrix} K_{uu} & K_{uT} \\ K_{Tu} & K_{TT} \end{bmatrix} \begin{Bmatrix} \Delta u \\ \Delta T \end{Bmatrix} = \begin{Bmatrix} R_u \\ R_T \end{Bmatrix} \tag{1}$$

where K is the coupled temperature-displacement Jacobi matrix; Δu and ΔT are the incremental displacement and temperature; R_u and R_T are the mechanical and thermal residual vectors.

The controlling differential equation for transient heat transfer in a wellbore is as follows.

$$c\rho \frac{\partial T}{\partial t} - \frac{\partial}{\partial x}\left(k_x \frac{\partial T}{\partial x} \right) - \frac{\partial}{\partial y}\left(k_y \frac{\partial T}{\partial y} \right) = 0 \tag{2}$$

where ρ is the density, kg/m^3; c is the specific heat capacity, J/(kg·K); k is the thermal conductivity, W/(m·K); T is the temperature, ℃; t is the time, s.

2.2 Cement sheath constitutive model

The theoretical basis of the plastic damage model is the continuum damage mechanics(George et al., 2017). Fig. 1 show the uniaxial tensile and compressive full stress-strain curves for cement.

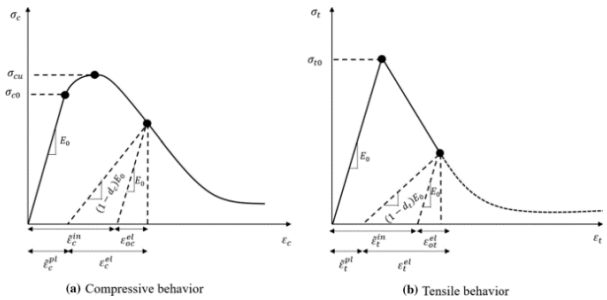

Figure 1. Response of cement to uniaxial loading in tension (a) and compression (b).

The uniaxial tensile and compressive stress-strain relations of cement are:

$$\begin{cases} \sigma_t = (1-d_t) E_0 \left(\varepsilon_t - \tilde{\varepsilon}_t^{pl} \right) \\ \sigma_c = (1-d_c) E_0 \left(\varepsilon_c - \tilde{\varepsilon}_c^{pl} \right) \end{cases} \tag{3}$$

The formulas for calculating the tensile and compressive damage factors of cement are as follows:

$$\begin{cases} d_{\mathrm{t}} = 1 - \dfrac{\sigma_{\mathrm{t}}}{E_0 \tilde{\varepsilon}_{\mathrm{t}}^{\mathrm{pl}} \left(1/b_{\mathrm{t}} - 1 \right) + \sigma_{\mathrm{t}}} \\ d_{\mathrm{c}} = 1 - \dfrac{\sigma_{\mathrm{c}}}{E_0 \tilde{\varepsilon}_{\mathrm{c}}^{\mathrm{pl}} \left(1/b_{\mathrm{c}} - 1 \right) + \sigma_{\mathrm{c}}} \end{cases} \tag{4}$$

The yield function of the plastic-damage concrete model is as follow.

$$F\left(\bar{\boldsymbol{\sigma}},\tilde{\varepsilon}^{pl}\right)=\frac{1}{1-\alpha}\left(\bar{q}-3\alpha\bar{p}+\beta\left(\tilde{\varepsilon}^{pl}\right)\hat{\bar{\sigma}}_{\max}-\gamma-\hat{\bar{\sigma}}_{\max}\right)-\bar{\sigma}_{c}\left(\tilde{\varepsilon}_{c}^{pl}\right)\leq 0 \tag{5}$$

where α and γ are dimensionless material constants.

3 NUMERICAL MODEL

3.1 Modeling

In this paper, the actual parameters of the Weiyuan W201-H3 shale well in China were selected for cement sheath integrity analysis. The outer diameter of the casing is 139.7 mm, the thickness is 10.54 mm and the borehole diameter is 215.9 mm. To eliminate boundary effects as far as possible, the overall size of the model is 1.5 x 1.5 m. As the casing, cement and formation are all axisymmetric, a two-dimensional 1/4 casing-cement-formation numerical model is developed. The cement interfaces adopt cohesive contact, as shown in Fig. 2. The normal displacement outside the model is fixed, and symmetry constraints are imposed on the symmetry boundary. The temperature on the outer boundary of the model maintains the initial temperature of the formation, and convective heat transfer occurs between the inner wall of the casing and the fracturing fluid. The internal wall of the casing is subjected to varying pressures to simulate the operations of injection/fracturing and shut-in.

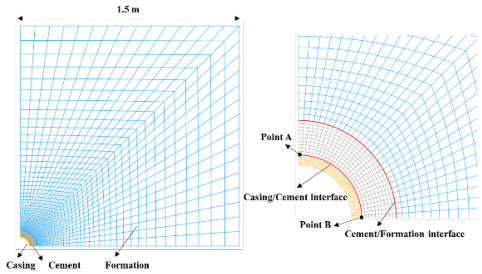

Figure 2. Geometric model of cement sheath Integrity.

3.2 *Material properties*

The casing is defined as a linear elastic material and the formation as an elasto-plastic material. The CDP model is used for the cement. Uniaxial compression and tension full stress-strain curves of the cement are first obtained, then damage parameters are calculated and finally input into the plastic damage model. The interface are modeled using zero-thickness cohesive contact.(Yin et al., 2019)

Table 1. Material properties for the casing, cement, and formation.

Materials		Casing	Cement	Rock
Modulus	[GPa]	210	7	30
Poisson's	[-]	0.3	0.23	0.25
Friction angle	[°]	-	27	30
Cohesion	[MPa]	-	10	20
Uniaxial tensile strength	[MPa]	-	2.2	-
Uniaxial compressive strength	[MPa]	-	25.1	-

3.3 *Model validation*

To verify the accuracy of the method, the results of numerical simulations are compared with physical experiments. Vrålstad et al. (2019) conducted an experimental study on the cement sheath integrity during pressure cycling. The experimental setup and numerical model are shown in the Fig. 3.

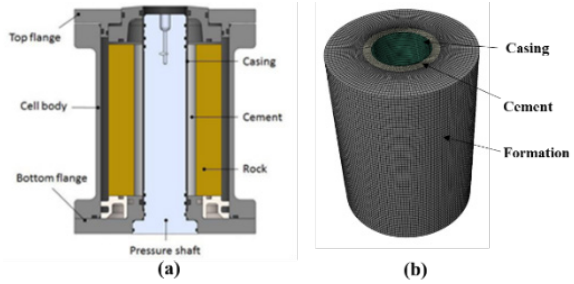

Figure 3. Cement sheath integrity model; (a) experimental setup; (b) Numerical model.

Fig. 4(a) shows the experimental results. As the casing internal pressure reaches 150 bar, small radial cracks begin to develop inside the cement. When the casing pressure is increased to 300 bar, the cement experiences catastrophic cracking. Fig. 4(b) shows the numerical results. DAMAGET represents the tensile damage factor. The results indicate that the casing internal pressure is 16.3 MPa when the cement starts to experience tensile damage, and it is 32.4 MPa after the cement has fully experienced tensile damage. The numerical results agree well with the experimental results.

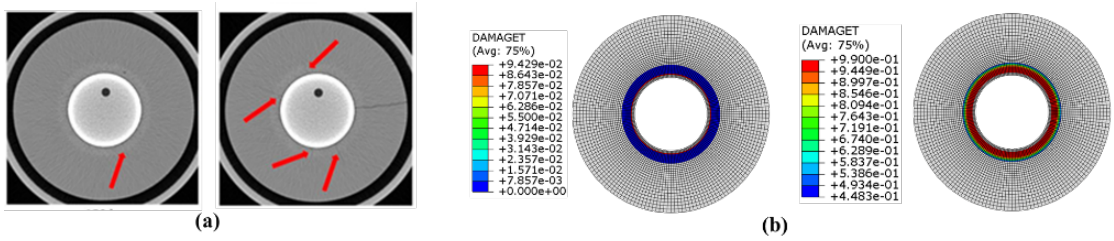

Figure 4. Model results; (a) CT images during pressure cycling; (b) Numerical results of tensile damage.

4 RESULTS AND DISCUSSIONS

In the W201-H3 shale well, the initial formation and fracturing fluid temperatures are 100 °C and 30 °C, respectively. The maximum internal casing pressure is 100 MPa. The hydraulic fracturing and shut-in times are 2 h and 1 h, respectively. The results are analysed in this section.

4.1 Temperature distribution

The wellbore temperature distribution during fracturing is shown in Fig. 5. As the fracturing time increases, the cement sheath temperature decreases. At the final moment of fracturing, the temperatures of the inside and outside of the cement are 32.9° and 62.8° respectively. As the shut-in time increases, the cement sheath temperature continued to rise. The temperatures of the inside and outside of the cement sheath rose to 73.5° and 76.4° at the final moment of shut-in operation.

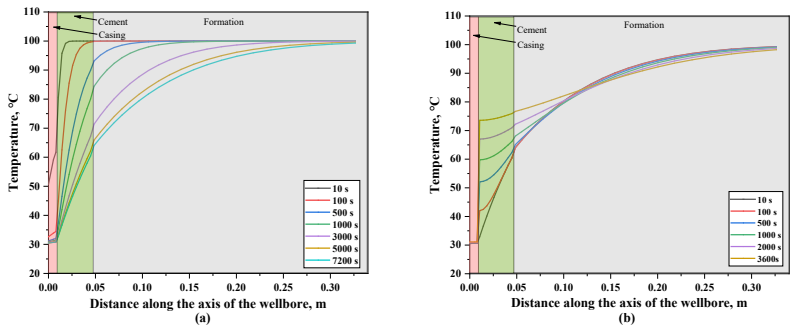

Figure 5. Temperature distribution along the wellbore axial direction; (a) fracturing; (b) shut-in.

4.2 Cement sheath damage

The tensile and compression damage factor reflects the degree of tensile and compression damage to the cement. Fig. 6 shows the damage factor of the cement sheath at the final moment of shut-in operation. The results show that the maximum tensile damage factor is 0.96, indicating that tensile damage has occurred inside the cement. The maximum compression factor is 0.04, indicating that compression damage to the cement is basically not occurring.

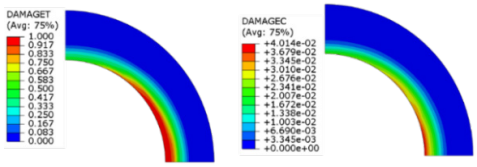

Figure 6. Tension and compression damage distribution of cement sheath.

Fig. 7 shows the damage factor inside the cement sheath. The results show that as the azimuth angle increases, the cement tensile and compression damage show a decreasing trend. The tensile damage factor of the cement is 0.94 and 0.49 for the azimuth angle of 0° and 90°, respectively.

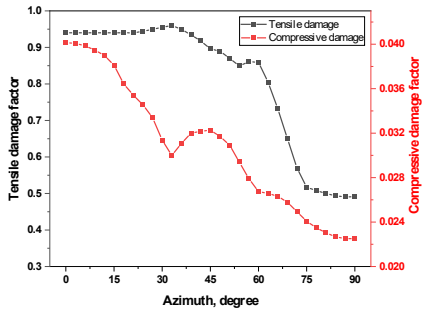

Figure 7. Variation of tensile and compressive damage inside the cement sheath with the azimuth.

4.3 Cement interface micro-annulus

The micro-annulus size is an important parameter reflecting the cement sheath seal integrity. Fig. 5 shows the change of the micro-annulus at point A and point B of the cement sheath interface over time, where point A and point B are marked in Fig. 2. After the shut-in operation, the pressure inside the casing drops rapidly. The casing/cement interface debond during the unloading process, and the maximum micro-annulus at point A reaches 39.57 μm. During the shut-in operation, the micro-annulus gradually decreased due to the thermal expansion of the cement sheath, and finally reached 38.69 μm. The maximum micro-annulus at point B is 25.10 μm, and finally decreased to 24.44 μm.

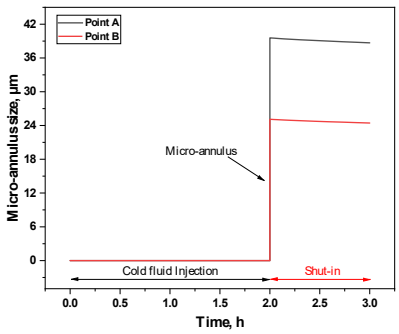

Figure 8. Micro-annulus during injection and shut-in.

5 CONCLUSIONS

In this paper, a 3D numerical model is developed to assess the cement sheath integrity considering thermal-mechanical coupling. The main conclusions are as follows.

1. The cement temperature decreases with increasing fracturing time. Due to the absence of low-temperature fluid flow, the cement temperature gradually increases with the increase in shut-in time.

2. The tensile damage occurs on the inside of the cement under higher casing internal pressure. The degree of tensile damage is larger in the direction of the maximum horizontal in-situ stress.

3. The casing-cement interface is subject to debonding during the unloading of the shut-in operation, with a maximum micro-annulus of 39.57 μm. During shut-in, the micro-annulus gradually decreases due to the thermal expansion of the cement, eventually falling to 38.69 μm.

REFERENCES

Arjomand, E., Bennett, T., & Nguyen, G. D. (2018). Evaluation of cement sheath integrity subject to enhanced pressure. Journal of Petroleum Science and Engineering, 170, 1–13. https://doi.org/10.1016/j.petrol.2018.06.013

De Andrade, J., & Sangesland, S. (2016a). Cement Sheath Failure Mechanisms: Numerical Estimates to Design for Long-Term Well Integrity. Journal of Petroleum Science and Engineering, 147, 682–698. https://doi.org/10.1016/j.petrol.2016.08.032

De Andrade, J., & Sangesland, S. (2016b). Cement Sheath Failure Mechanisms: Numerical Estimates to Design for Long-Term Well Integrity. Journal of Petroleum Science and Engineering, 147, 682–698. https://doi.org/10.1016/j.petrol.2016.08.032

Feng, Y., Li, X., & Gray, K. E. (2017). Development of a 3D numerical model for quantifying fluid-driven interface debonding of an injector well. International Journal of Greenhouse Gas Control, 62, 76–90. https://doi.org/10.1016/j.ijggc.2017.04.008

George, J., Kalyana Rama, J. S., Siva Kumar, M. V. N., & Vasan, A. (2017). Behavior of Plain Concrete Beam subjected to Three Point Bending using Concrete Damaged Plasticity (CDP) Model. Materials Today: Proceedings, 4(9), 9742–9746. https://doi.org/10.1016/j.matpr.2017.06.259

Gu, C., Li, X., Feng, Y., Deng, J., & Gray, K. (2022). Numerical investigation of cement interface debonding in deviated shale gas wells considering casing eccentricity and residual drilling fluid. International Journal of Rock Mechanics and Mining Sciences, 158, 105197. https://doi.org/10.1016/j.ijrmms.2022.105197

Guo, B., Shan, L., Jiang, S., Li, G., & Lee, J. (2018). The maximum permissible fracturing pressure in shale gas wells for wellbore cement sheath integrity. Journal of Natural Gas Science and Engineering, 56, 324–332. https://doi.org/10.1016/j.jngse.2018.06.012

Li, J., Xi, Y., Tao, Q., Li, Y., & Qu, G. (2020). Experimental investigation and numerical simulation of the emergence and development of micro-annulus in shale gas wells subjected to multistage fracturing. Journal of Natural Gas Science and Engineering, 78, 103314. https://doi.org/10.1016/j.jngse.2020.103314

Thiercelin, M. J., Dargaud, B., Baret, J. F., & Rodriquez, W. J. (1998). Cement design based on cement mechanical response. SPE Drilling & Completion, 13(04), 266–273.

Vrålstad, T., Skorpa, R., & Werner, B. (2019, March 4). Experimental Studies on Cement Sheath Integrity During Pressure Cycling. SPE/IADC International Drilling Conference and Exhibition. https://doi.org/10.2118/194171-MS

Yan, X., Jun, L., Gonghui, L., Qian, T., & Wei, L. (2018). A new numerical investigation of cement sheath integrity during multistage hydraulic fracturing shale gas wells. Journal of Natural Gas Science and Engineering, 49, 331–341. https://doi.org/10.1016/j.jngse.2017.11.027

Yin, F., Hou, D., Liu, W., & Deng, Y. (2019). Novel assessment and countermeasure for micro-annulus initiation of cement sheath during injection/fracturing. Fuel, 252, 157–163. https://doi.org/10.1016/j.fuel.2019.04.018